

## MIT Open Access Articles

*Optimizing Electrode Configuration for Electrical Impedance Measurements of Muscle via the Finite Element Method*

The MIT Faculty has made this article openly available. **Please share** how this access benefits you. Your story matters.

**Citation:** Jafarpoor, Mina, Jia Li, J. K. White, and S. B. Rutkove. "Optimizing Electrode Configuration for Electrical Impedance Measurements of Muscle via the Finite Element Method." IEEE Trans. Biomed. Eng. 60, no. 5 (May 2013): 1446–1452.

**As Published:** <http://dx.doi.org/10.1109/TBME.2012.2237030>

**Publisher:** Institute of Electrical and Electronics Engineers (IEEE)

**Persistent URL:** <http://hdl.handle.net/1721.1/91024>

**Version:** Author's final manuscript: final author's manuscript post peer review, without publisher's formatting or copy editing

**Terms of use:** Creative Commons Attribution-Noncommercial-Share Alike





Published in final edited form as:

*IEEE Trans Biomed Eng.* 2013 May ; 60(5): 1446–1452. doi:10.1109/TBME.2012.2237030.

## Optimizing Electrode Configuration for Electrical Impedance Measurements of Muscle via the Finite Element Method

**Mina Jafarpoor, BS,**

Department of Neurology, Beth Israel Deaconess Medical Center, Harvard Medical School, Boston, MA 02215, USA

**Jia Li, PhD,**

Department of Neurology, Beth Israel Deaconess Medical Center, Harvard Medical School, Boston, MA 02215, USA

**Jacob K. White, PhD, and**

Department of Electrical Engineering and Computer Science, Massachusetts Institute of Technology, 55 Massachusetts Ave, Cambridge, MA 02139 USA (white@mit.edu)

**Seward B. Rutkove, MD**

Department of Neurology, Beth Israel Deaconess Medical Center, Harvard Medical School, Boston, MA 02215, USA

### Abstract

Electrical impedance myography (EIM) is a technique for the evaluation of neuromuscular diseases, including amyotrophic lateral sclerosis and muscular dystrophy. In this study, we evaluated how alterations in the size and conductivity of muscle and thickness of subcutaneous fat impact the EIM data, with the aim of identifying an optimized electrode configuration for EIM measurements. Finite element models were developed for the human upper arm based on anatomic data; material properties of the tissues were obtained from rat and published sources. The developed model matched the frequency-dependent character of the data. Of the three major EIM parameters, resistance, reactance, and phase, the reactance was least susceptible to alterations in the subcutaneous fat thickness, regardless of electrode arrangement. For example, a quadrupling of fat thickness resulted in a 375% increase in resistance at 35 kHz but only a 29% reduction in reactance. By further optimizing the electrode configuration, the change in reactance could be reduced to just 0.25%. For a fixed 30 mm distance between the sense electrodes centered between the excitation electrodes, an 80 mm distance between the excitation electrodes was found to provide the best balance, with a less than 1% change in reactance despite a doubling of subcutaneous fat thickness or halving of muscle size. These analyses describe a basic approach for further electrode configuration optimization for EIM.

### Index Terms

Neuromuscular disease; electrical impedance; subcutaneous fat; muscle

### I. Introduction

Electrical impedance myography (EIM) is a four-electrode bioelectrical impedance-based technique for the assessment of diseases affecting nerve and muscle [1]. The technique is

effective for monitoring disease status, including the impact of drug therapy and could serve as a useful outcome measure in clinical trials [2]. It also holds promise as a method to assist in the initial diagnosis of neuromuscular disease [3]. Advantages of EIM over standard approaches such as needle electromyography (EMG) include that the technique is painless, non-invasive, and quantitative, thus providing metrics that can be followed over time to see how well a condition is responding to treatment. EIM is also sensitive to disuse atrophy [4], a condition that EMG cannot assess effectively. Since EIM measurements rely upon the localized flow of electrical current through muscle tissue, the technique is dependent on a variety of spatial and volumetric factors, some under experimental control and others not. For example, the size and shape of the muscle as well as the orientation of the muscle fibers will impact the data. Non-muscular anatomic factors can also influence the data, including the overall size of the limb and the amount of subcutaneous fat. Finally, the obtained data is highly dependent on the choice of electrode size and inter-electrode distances. Therefore, it will ultimately be critical to standardize electrode parameters if EIM is to be widely employed as a clinical or research tool.

To date, many of the clinical studies employing EIM have focused on following disease status over time [1, 5]. If only the muscle is changing and the skin, subcutaneous fat and bone are stable, alterations in the measured impedance values can be taken as being due mostly to alterations in the size or the material properties of the muscle. However, if we are interested in also comparing data across individuals rather than only longitudinally over time, it is then necessary to evaluate the impact of these other tissues and to identify approaches for minimizing them.

We have previously employed the finite element method (FEM) as a means for evaluating the relationship between surface EIM data and the electrical properties of the surrounding tissues in the rat gastrocnemius muscle [6]. In this study, we extend those initial efforts by assessing how changes in geometric factors impact the measured impedance data in the human biceps brachii muscle. The goal is to help identify which impedance parameters and which electrode configurations are least impacted by variations in subcutaneous fat and muscle thickness, while still being sensitive to the expected changes in muscle material properties induced by neuromuscular disease.

## II. Materials and Methods

### A. Human Anatomic and Impedance Data

Beth Israel Deaconess Medical Center's institutional review board approved all human studies, and the subject provided written informed consent.

Raw morphological and surface impedance data were obtained from a healthy 47-year-old male. Biceps girth was obtained using a tape measure around several points of the upper arm, including the area of maximal girth, measured at 295 mm. The subcutaneous fat thickness overlying biceps at this maximal point, measured with a Terason 2000 system (Teratech, Inc, Burlington MA), was 4.4 mm.

Surface impedance measurements from 3 kHz to 500 kHz were made using the Imp SFB7® (Impedimed, Inc, Sydney, Australia). Surface adhesive electrodes (Product# 019-435500, Nicolet Biomedical, Madison, WI), size  $25 \times 7$  mm, was cut to  $\frac{1}{2}$  length ( $12.5 \times 7$  mm), and placed in a pattern identical to that used in a handheld probe [7]: 30 mm between the two inner sense electrodes and a total of 60 mm between the two outer excitation electrodes (i.e., each excitation electrode placed 15 mm peripheral to each of the sense electrodes). These electrode positions and sizes had been chosen arbitrarily, but with the goal of fitting readily

over the muscle. Impedance measurements were made in a relaxed posture with the elbow bent at 90 degrees resting on the subject's lap.

From the raw reactance ( $X$ ) and resistance ( $R$ ) values, the phase ( $\theta$ ) was calculated via the relationship  $\theta = \arctan(X/R)$ . In order conform to the standard bioimpedance convention, all reactance and phase values are plotted as positive values rather than negative.

## B. Animal Impedance Data

Since human muscle tissue was not available from which to measure dielectric data, muscle was obtained from gastrocnemius muscle of 14 healthy rats of 14 to 15 weeks of age. All animal procedures were approved by Beth Israel Deaconess Medical Center's Institutional Animal Care and Use Committee.

Immediately after sacrifice, the tissue was removed and cut into a slab with a  $10 \times 10$  mm base and approximately 4 mm height. This was placed in a custom impedance measuring cell [8]. The impedance of the tissue was measured from 500 Hz to 1 MHz, using an impedance-measuring system consisting of a multifrequency lock-in amplifier (Model 7280, Signal Recovery, Oak Ridge, TN) sampling at 7.5 MHz coupled with a very low-capacitance active probe (Model 1103 of Tektronix, Beaverton, OR), as has been previously described [6]. Impedance values were used to extract the permittivity and conductivity for each individual rat muscle. In order to account for the muscle's anisotropy in the model, measurements were made on the muscle in both the longitudinal and transverse directions relative to the muscle fiber direction [9]. Results were then averaged over all of the animals.

## C. Finite Element Model of the Upper Arm

The model was developed and analyzed using the AC/DC Module, Electric Currents Physics, in Comsol Multiphysics software (Comsol, Inc, 4.2a Burlington, MA). The proximal end of the model extended toward the axilla and the distal end extended just proximal to the antecubital fossa (Fig. 1). The model consisted of skin-subcutaneous fat, cortical bone (humerus), marrow and several muscles: biceps, brachialis, and triceps. Only the metallic surface of the electrode was modeled; no inter-electrode capacitances or contact impedances were included (the latter being likely inconsequential at the frequencies of interest as they are several orders of magnitude smaller than the input impedance of the voltage sensors). The baseline inter-electrode distances were 15mm-30mm-15mm, following the same pattern as that used on the subject. The muscle and tissue material properties were homogeneous throughout the model. For non-electrode boundaries, the normal component of the electric current was assumed to be continuous. Electrodes were modeled as potential surfaces the boundaries of which had either the excitation or zero current, except for the ground electrode, the potential of which was fixed at zero volts. The discretization mesh was generated automatically with the Comsol software. The final meshes for the model consisted of 13032 tetrahedral elements with an 8 s solution time.

At each measured frequency, longitudinal and transverse conductivities and permittivities were obtained from the rat studies and were incorporated into the model with rat data substituting for the normal human muscle. Fat, cortical bone and marrow were obtained over the frequency spectrum from Gabriel's dielectric survey and the associated online resources [10]. The skin-subcutaneous fat, cortical bone and marrow were all assumed to be isotropic.

After solving the finite element problem for the model, the voltage between the midpoints of the two sense electrodes was calculated and effective impedance values extracted as previously described [6].

Several variations to the model were then made, including altering subcutaneous fat thickness, muscle conductivity and thickness, and electrode configuration, while leaving the permittivity values unchanged. These changes were described as a baseline multiple (e.g., 2× indicates twice the thickness; 0.75× means 25% thinner).

### III. Results

#### A. Comparing FEM Values with the Measured EIM Values

Figure 2 compares the surface recorded human data and the FEM-generated data. As can be seen, the overall character of the curves is similar although there is an offset for both the reactance and the resulting phase angle values.

#### B. Modeling Changes in Subcutaneous Fat Thickness

We first assessed how alterations in subcutaneous fat thickness affected the measured results. Using the FEM model, we decreased the base subcutaneous fat thickness of 4.4 mm by 0.5× and increased it up to 4×—to a total depth of 17.6 mm. We chose this range since it is typical of human variation. The results of these analyses are shown in Figure 3. As can be seen both for resistance and phase, there is a very strong dependence on the skin-subcutaneous fat thickness, across the frequency spectrum. However, reactance appears relatively less affected, demonstrating considerably smaller changes in the frequency range of interest (approximately 10–150 kHz), as shown in Table 1. For example, at the peak reactance value of 35 kHz, a quadrupling of the subcutaneous fat thickness from 4.4 mm to 17.6 mm resulted in reactance decreasing from 28.8 to 20.5 ohms, a change of 29%. In comparison, at the same frequency, a quadrupling of the subcutaneous fat resulted in an increase in resistance from 79.9 to 379 ohms, an increase of 375%. (See also Table 1.)

#### C. Effect of Altering Muscle Size

We next decreased and increased the radius of the muscle from 0.5× to 1.5×. Such variation in size is commonly observed in healthy individuals. The resulting alterations in the impedance spectrum are shown in Figure 4. In this case, the measurements were not substantially impacted until the muscle was reduced to one half its original size. Of interest, the phase appeared to be least impacted by muscle size, consistent with previous observations [11].

#### D. Alerting the Inter-electrode Distances

We next evaluated a second electrode configuration, with the excitation electrodes placed at a greater distance from the sense electrodes (35 mm as compared to 15 mm) while maintaining the 30 mm separation in the sense electrodes, thus making entire array 100 mm in length. We then repeated the identical analyses (Figures 5 and 6). As can be seen, the subcutaneous fat had a much smaller impact on all three measures; most notably, there was only a very modest effect on the measured reactance; the resistance and phase values were also considerably less affected by the change in fat thickness. For example, with a quadrupling of the fat thickness, the peak reactance at 35 kHz changed just 0.25%, increasing from 13.41 ohms to 13.44 ohms. In contrast, the effect on muscle size appears considerably greater. (See also Table 1.)

#### E. Comparing Inter-electrode Distances

Figures 7 and 8 study how different subcutaneous fat and muscle thicknesses impact the three measured parameters at 35 kHz at different inter-electrode distances plotted relative to the baseline muscle and fat thickness. Although there is clearly no ideal position, with the excitation electrodes placed 80 mm apart the measured reactance is only modestly affected

by the subcutaneous fat thickness and muscle size. Figure 9 shows the current densities for the three electrode arrays, demonstrating the substantially larger volume through which the current flows when the electrodes are spaced further apart.

A final question remains whether the surface impedance parameters are affected by different inter-electrode distances if the muscle properties themselves change. Previous work has shown that muscle conductivity can change considerably in neuromuscular disease [8, 12]. Thus, Figure 10 summarizes the data for the 3 electrode arrangements for 2 different conductivities relative to a baseline value of 0.6 S/m and the baseline subcutaneous fat thickness of 4.4 mm, showing that changing the inter-electrode distance produces only a slight alteration in the measured resistance, reactance and phase, whether the conductivity is 1.5× normal (0.9 S/m) or half normal (0.3 S/m).

## IV. Discussion

There are three major results to this study. First, of the three impedance parameters, reactance, resistance, and phase, reactance appears by far least affected by alterations in the subcutaneous fat thickness. Second, of the electrode configurations tested here, for a fixed inter-sense electrode distance of 30 mm, a separation of 80 mm in the excitation electrodes provides the best compromise for minimizing the effects of muscle size and subcutaneous fat thickness. Finally, the measured conductivity of the muscle is relatively unaffected by the inter-electrode distance, suggesting that whichever set-up works best from a subcutaneous fat and muscle thickness standpoint would still be sufficient to detect changes the material properties of muscle induced by neuromuscular disease.

Early work in EIM employed the use of excitation electrodes placed far from the sense electrodes (for example placed on the palms of both hands with the sense electrodes placed on a unilateral biceps) [13]. This had the advantage of ensuring that the subcutaneous fat had only a minimal impact on the data [14], since the electrical current was primarily traveling through the more conductive muscle at the point of measurement. However, this method had a variety of drawbacks. For example, even small alterations in joint position had a major impact on the data and a variety of muscles could not be measured due to the need to have the electrodes so far apart; moreover, the entire measurement system could not be contained within a small footprint, making measurements slow and inconvenient to perform. Finally, such an approach also made it impossible to measure the anisotropic properties of the muscle *in vivo* [3]. For these reasons, we began performing EIM with the excitation electrodes in relatively close proximity to the sense electrodes.

The one major drawback with this approach, however, is that the thickness of the subcutaneous fat would be expected to play a much greater role in the obtained impedance values. Thus, we became interested in the relationship between inter-electrode distance and the measured impedance values at different subcutaneous fat thicknesses.

An additional challenge is the change in muscle size that can occur both in neuromuscular disease but also due to normal variation in anatomy. Importantly, the fact that the EIM data is affected by changes in muscle size is not altogether problematic, since we anticipate that alterations in muscle size are part of the reason that EIM is very sensitive to a variety of neuromuscular conditions as most disorders are accompanied by substantial muscle fiber atrophy and consequently a loss in the overall size of the muscle. These morphometric impedance changes generally move in the same direction as those due to the alteration of the electrical parameters themselves. Regardless of the details, understanding the relationship of the impedance data and muscle size can explain some of the observed normal variation in impedance data among healthy individuals.

An additional question that arises is whether by moving the excitation electrodes far apart we are still able to detect alterations in the conductivity if there is considerable overlying fat, or if the signal would be lost since the electrical current would become too diffuse.

Additional modeling, not detailed here, found that even under these circumstances, by spacing the excitation electrodes further apart we still achieve good sensitivity to change, consistent with our overall interpretation of the data. For example, with subcutaneous fat set at  $4.0\times$  baseline and an inter-electrode distance of 100mm for the excitation electrodes, a 20% increase in conductivity still yields a 7.5% decrease in the measured phase value.

Regardless of the size of the muscle or subcutaneous fat, of the three major EIM values, the reactance appears least affected by alterations in the subcutaneous fat thickness, only decreasing by about 21% with a nearly 4-fold increase in fat at 35 kHz with the more compact electrode arrangement and only 0.25% with the larger 100 mm arrangement. In comparison, resistance increases nearly 375% with a 4-fold increase in fat thickness with the tighter electrode arrangement but still increases 179% with the electrodes further apart. Of interest, the major variable that we have been utilizing in much of our work, the phase, is also severely affected by the subcutaneous fat thickness when using the tighter configuration.

One other issue of interest is how “good” a variable the reactance is. In fact, in studies where we have specifically assessed the reactance, it appears to be very sensitive to disease status [15]; however, since the reactance values are considerably smaller than that of the resistance, it does tend to be a noisier parameter. Clearly, going forward it will be important to continue to assess the value of both the reactance and phase in ongoing animal and human studies.

In this analysis, we have performed the most basic of comparisons focusing only on the muscle and subcutaneous fat thickness independently. Clearly, these 2 parameters may change simultaneously along with changes in the conductivity. Thus, the reality of the situation is far more complex than suggested here. Moreover, to simplify the analyses, we have kept the sense electrode distance unchanged at 30 mm. Thus, this group of analyses serves only as a foundation for a more generalized approach for identifying the impact of a variety of factors on the measured impedance of the muscle. For example, by reducing the distance between the sense electrodes, it is possible that we could keep the overall size of the array much smaller while still reducing the impact of the subcutaneous fat.

One final important point is that these analyses are also limited by our having used rat muscle tissue and an online database for the dielectric values in these analyses rather than those from fresh human tissue; as Figure 2 demonstrates, although these values mirror the overall frequency-dependent behavior of the observed data, they do not accurately reflect the absolute values themselves. Thus, the results of this entire study are an approximation of those that would be anticipated to occur with real-world measurements in humans.

## V. Conclusion

Using FEM, we have explored the effects of a varying subcutaneous fat and muscle thickness on the measured impedance data in a human biceps model. While it is clear that all 3 impedance parameters are impacted by increasing thickness of the subcutaneous fat, the reactance is the least sensitive to this effect at the frequencies of apparent greatest interest, between approximately 10 and 300 kHz. In addition, variations in muscle size appear to play a more modest role in the obtained data, although it too has important effects and could account for variations in surface measured impedances amongst healthy individuals. Most importantly, based on this analysis, it is clear that alterations in the electrode configuration

can greatly impact the data and its sensitivity to morphological variation. For a fixed 30 mm inter-electrode distance of the sense electrodes, an 80 mm spacing between excitation electrodes appears to give the best compromise in terms of reduced sensitivity to subcutaneous fat thickness and muscle size. Importantly, changes in the surface measured impedance values induced by alterations in muscle conductivity values, a consequence of neuromuscular disease, are only modestly affected by inter-electrode distance. Further refinement of electrode configurations are needed to optimize EIM for clinical use; this will only be achieved with further modeling and detailed study of human subjects.

## Acknowledgments

The authors acknowledge the assistance of Tom Geisbush in the preparation of this manuscript.

This work was supported by the National Institutes of Health/National Institute of Neurological Diseases and Stroke, Grant R01-055099 and the Singapore-MIT program in computational engineering.

## References

1. Rutkove SB. Electrical Impedance Myography: Background, Current State, and Future Directions. *Muscle Nerve*. 2009; vol. 40:936–946. [PubMed: 19768754]
2. Rutkove SB, Zhang H, Schoenfeld DA, Raynor EM, Shefner JM, Cudkowicz ME, Chin AB, Aaron R, Shiffman CA. Electrical impedance myography to assess outcome in amyotrophic lateral sclerosis clinical trials. *Clin Neurophysiol*. 2007 Nov.vol. 118:2413–2418. [PubMed: 17897874]
3. Garmirian LP, Chin AB, Rutkove SB. Discriminating neurogenic from myopathic disease via measurement of muscle anisotropy. *Muscle Nerve*. 2009 Jan.vol. 39:16–24. [PubMed: 19058193]
4. Tarulli AW, Duggal N, Esper GJ, Garmirian LP, Fogerson PM, Lin CH, Rutkove SB. Electrical impedance myography in the assessment of disuse atrophy. *Arch Phys Med Rehabil*. 2009 Oct.vol. 90:1806–1810. [PubMed: 19801075]
5. Glass D, Roubenoff R. Recent advances in the biology and therapy of muscle wasting. *Annals of the New York Academy of Sciences*. 2010; vol. 1211:25–36. [PubMed: 21062293]
6. Wang LL, Ahad M, McEwan A, Li J, Jafarpoor M, Rutkove SB. Assessment of alterations in the electrical impedance of muscle after experimental nerve injury via finite-element analysis. *IEEE transactions on bio-medical engineering*. 2011 Jun.vol. 58:1585–1591. [PubMed: 21224171]
7. Narayanaswami P, Spieker AJ, Mongiovi P, Keel JC, Muzin SC, Rutkove SB. Utilizing a handheld electrode array for localized muscle impedance measurements. *Muscle Nerve*. 2012 (in press).
8. Ahad MA, Fogerson PM, Rosen GD, Narayanaswami P, Rutkove SB. Electrical characteristics of rat skeletal muscle in immaturity, adulthood, and after sciatic nerve injury and their relation to muscle fiber size. *Physiol Meas*. 2009; vol. 30:1415–1427. [PubMed: 19887721]
9. Epstein BR, Foster KR. Anisotropy in the dielectric properties of skeletal muscle. *Med Biol Eng Comput*. 1983 Jan.vol. 21:51–55. [PubMed: 6865513]
10. Institute of Applied Physics (IFAC). Dielectric properties of body tissues. 2007 Available: <http://niremf.ifac.cnr.it/tissprop/>.
11. Shiffman C, Aaron R, Altman A. Spatial dependence of the phase in localized bioelectrical impedance analysis. *Phys Med Biol*. 2001 Apr.vol. 46:N97–N104. [PubMed: 11324975]
12. Ahad MA, Narayanaswami P, Kasselmann LJ, Rutkove SB. The effect of subacute denervation on the electrical anisotropy of skeletal muscle: implications for clinical diagnostic testing. *Clin Neurophysiol*. 2010 Jun.vol. 121:882–886. [PubMed: 20153247]
13. Rutkove S, Aaron R, Shiffman C. Localized bioimpedance analysis in the evaluation of neuromuscular disease. *Muscle Nerve*. 2002 Mar.vol. 25:390–397. [PubMed: 11870716]
14. Tarulli AW, Chin AB, Lee KS, Rutkove SB. Impact of skin-subcutaneous fat layer thickness on electrical impedance myography measurements: An initial assessment. *Clin Neurophysiol*. 2007 Nov.vol. 118:2393–2397. [PubMed: 17889597]



15. Wang LL, Spieker AJ, Li J, Rutkove SB. Electrical impedance myography for monitoring motor neuron loss in the SOD1 G93A amyotrophic lateral sclerosis rat. *Clin Neurophysiol.* 2011; vol. 122:2505–2511. [PubMed: 21612980]

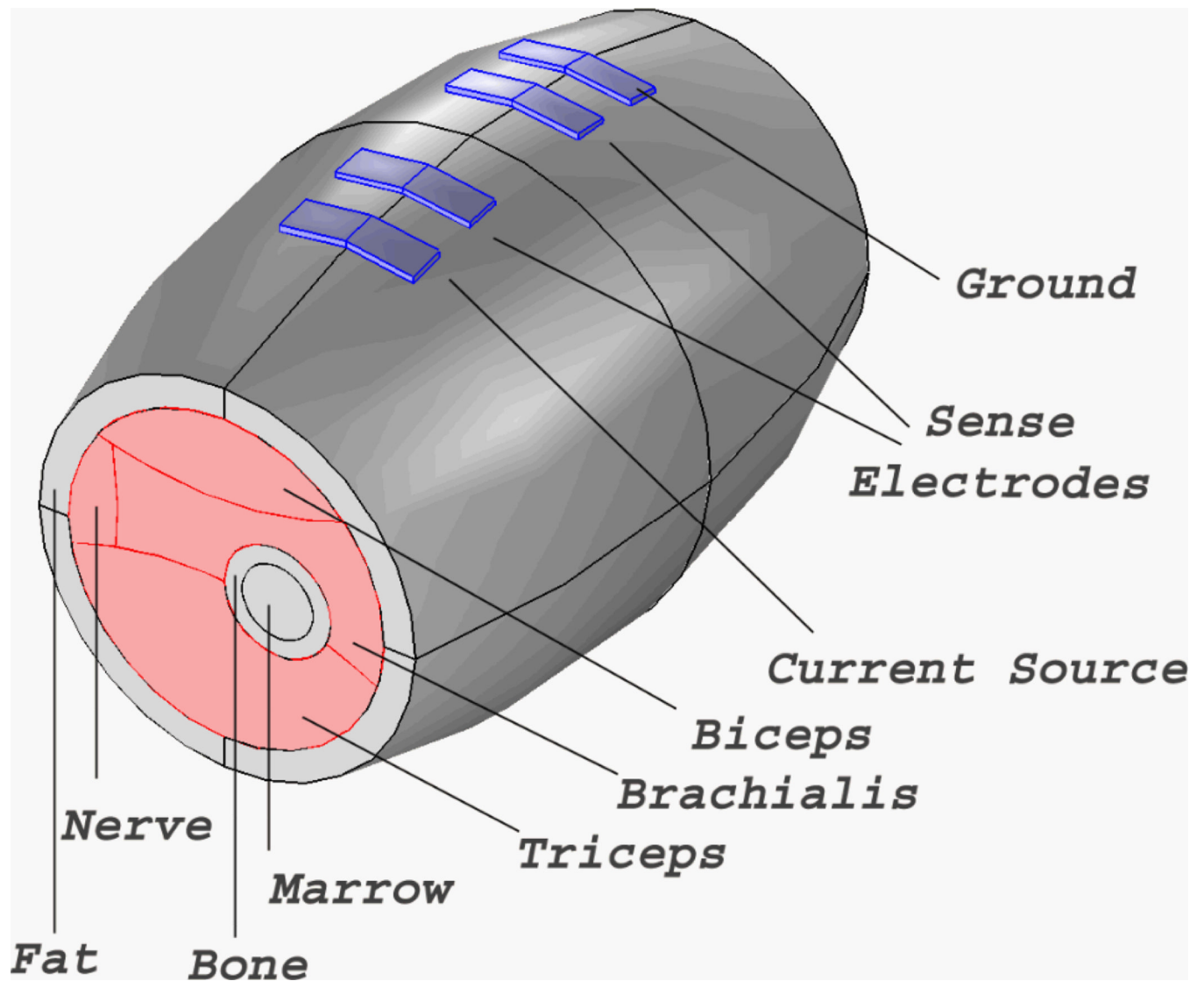


**Fig. 1.** FEM model of the human arm using Comsol Multiphysics 4.2a (elbow to axilla) based on anatomic data. The major muscle complexes, bones, and surface structures are identified. The inter-electrode spacing was 15 mm-30 mm-15 mm (60 mm in total).

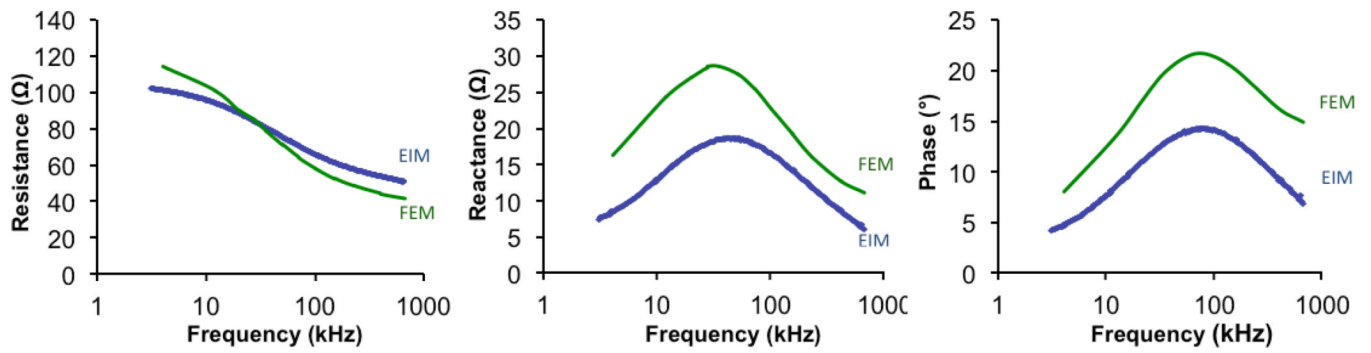


**Fig. 2.** Comparison of EIM data from 47-year-old healthy male volunteer (blue line) and that generated using FEM (green line). Although there is an offset in the reactance and resistance data, the frequency dependence of all three parameters of the model accurately mirrors the measured human data.

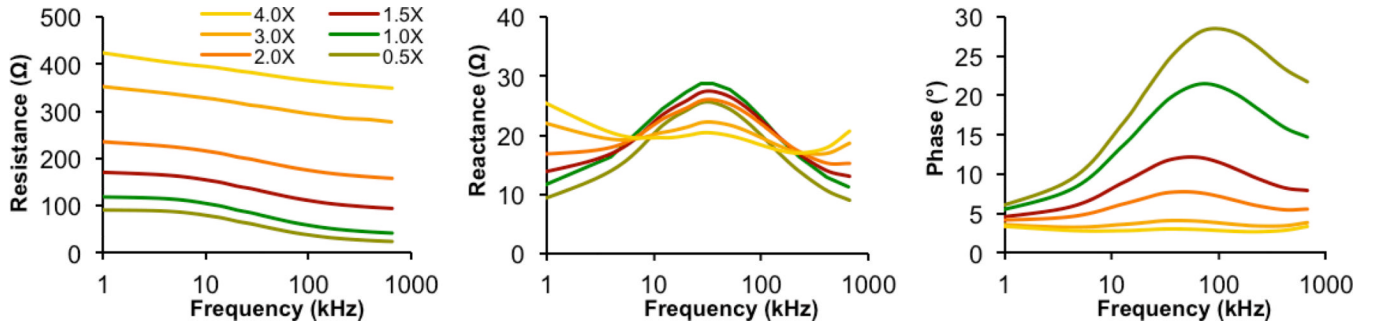


**Fig. 3.** The effect of altering the baseline 4.4 mm subcutaneous fat thickness on the resistance, reactance and phase. Thicknesses were input in a range from 2.2 mm to 17.6 mm using the electrode arrangement and spacing shown in Fig. 1. Note how the resistance and phase values show a very strong dependence on subcutaneous fat, whereas the reactance in the 10–150 kHz shows a more modest sensitivity.

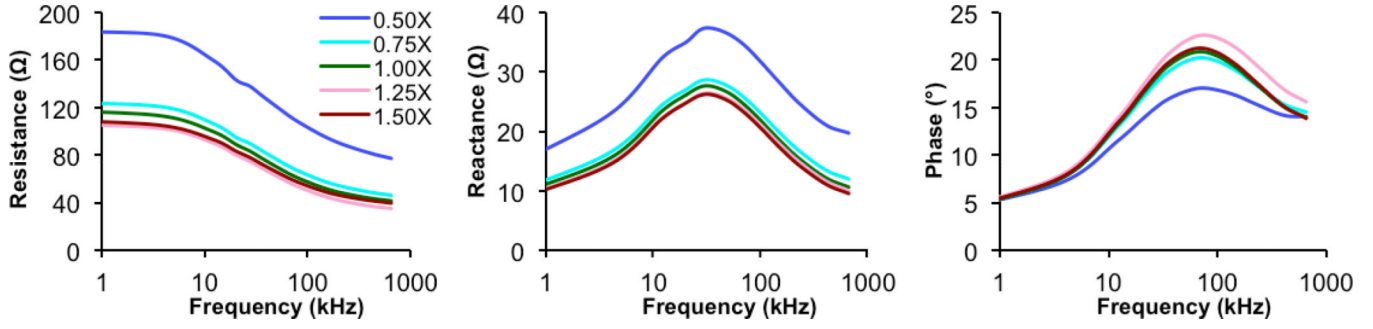


**Fig. 4.** The effect of altering the thickness of muscle on the measured impedance parameters using the electrode configuration and spacing shown in Fig. 1. As can be seen, unlike the case with subcutaneous fat thickness, only with marked reductions in size are the parameters substantially affected. Also, unlike with subcutaneous fat thickness, the phase appears least affected rather than reactance.

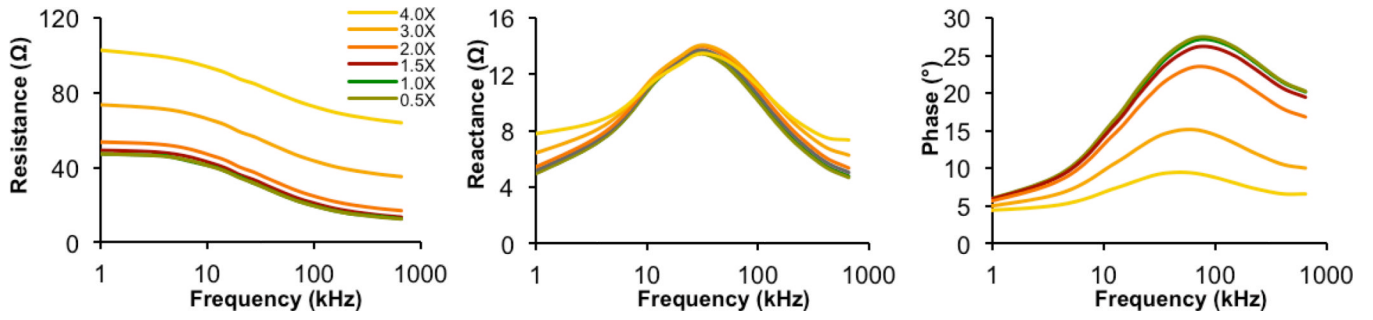


**Fig. 5.** Effect of altering subcutaneous fat thickness with each excitation electrode placed 2 cm further away from each sense electrode while keeping the sense interelectrode distance unchanged at 30 mm. Note how the impact on all three measures is greatly reduced as compared to the original spacing (Fig. 3); the reactance is virtually unchanged in the 10–100 kHz frequency range.

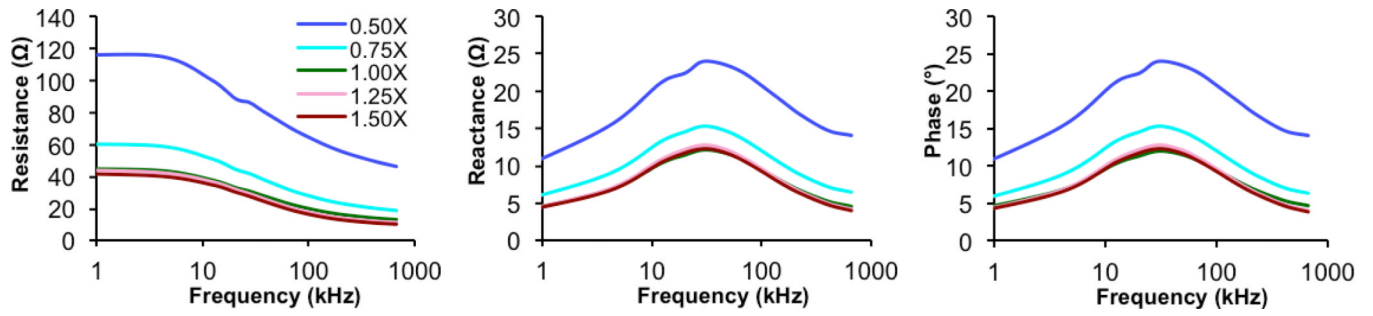


**Fig. 6.** The effect of altering muscle thickness at the greater inter-electrode distance. Note how all three parameters show a proportionally greater effect.

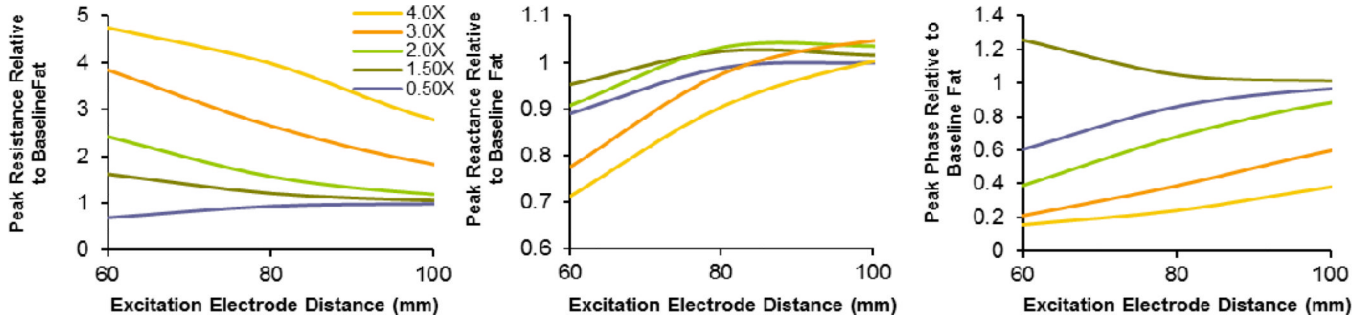


**Fig. 7.** The effect of inter-electrode distance on the measured 35 kHz resistance, reactance and phase values for several different thicknesses of subcutaneous fat relative to baseline (1.0). As can be seen, the greater the inter-electrode distance, the less the impact of the subcutaneous fat thickness; this effect is especially prominent for reactance.



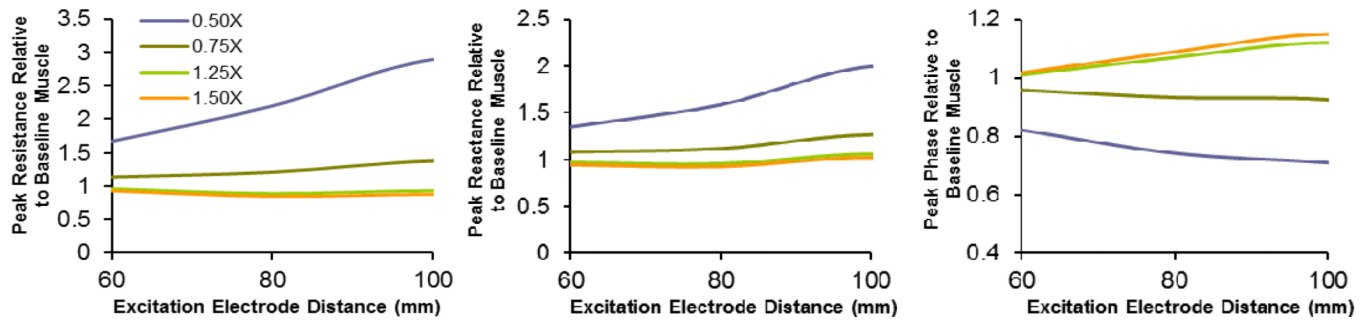


**Fig. 8.**

The effect of inter-electrode distance on the measured 35 kHz resistance, reactance and phase values for several different thicknesses of muscles relative to baseline (1.0). As can be seen, in contrast to the subcutaneous fat thickness above, the smaller the inter-electrode distance, the less the impact of muscle thickness. Taken together, the 80 mm inter-electrode distance may provide the best compromise.

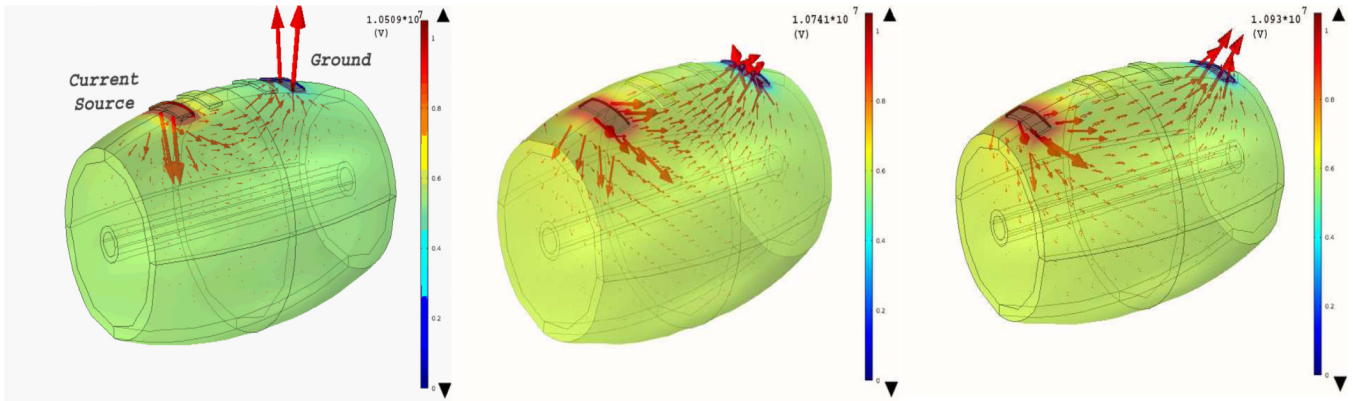


**Fig. 9.** Comparison of current distributions for the three different electrode configuration studies (15-30-15mm, 25-30-25mm, and 35-30-35mm). Note how the current distribution increases markedly as the excitation electrodes are placed further apart.

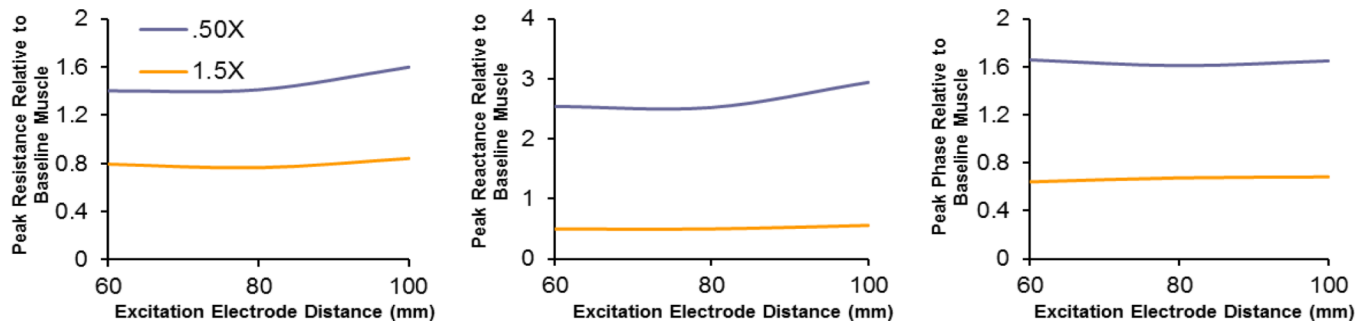


**Fig. 10.**

The effect of inter-electrode distance on the measured 35 kHz resistance, reactance and phase for 2 different conductivities relative to a baseline conductivity of 0.60 S/m. The changes in surface measured impedance values are only minimally affected by inter-electrode distances, regardless of the value of the conductivity.

**TABLE 1**

Resistance, Reactance and Phase at 35 KHz Frequency: the effect of increasing subcutaneous fat thickness with 2 different electrode arrangements

<b>Electrode Arrangement</b>	<b>Baseline thickness</b>	<b>2× thickness</b>	<b>4× thickness</b>
<b>Resistance (ohms)</b>			
<i>15-30-15 (60 mm)</i>	79.9	193 (+142%)	379 (+375%)
<i>35-30-35 (100 mm)</i>	29.5	35.1 (+19%)	82.3 (+179%)
<b>Reactance (ohms)</b>			
<i>15-30-15 (60 mm)</i>	28.8	26.1 (−9%)	20.4 (−29%)
<i>3.5-3-3.5 (100 mm)</i>	13.4	13.9 (+3.5%)	13.4 (+0.25%)
<b>Phase (°)</b>			
<i>1.5-30-15 (60 mm)</i>	19.79	7.68 (−62%)	3.08 (−85%)
<i>35-30-35 (100 mm)</i>	24.4	21.6 (−10%)	9.27 (−60%)